KEEVIL, C.E., CHANSON, H., and REUNGOAT, D. (2015)." Fluid Flow and Sediment Entrainment in the Garonne River Bore and Tidal Bore Collision." *Earth Surface Processes and Landforms*, Vol. 40, No. 12, pp. 1574-1586 (DOI: 10.1002/esp.3735) (ISSN 0197-9337).

FLUID FLOW AND SEDIMENT ENTRAINMENT IN THE GARONNE RIVER BORE AND TIDAL BORE COLLISION

Claire E. KEEVIL ([1]), Hubert CHANSON ([2]) and David REUNGOAT ([3])
([1]) Ph.D. Research Student, University of Hull, Department of Geography, Environment and Earth Sciences, Hull HU6 7RX, UK
(2) Professor, The University of Queensland, School of Civil Engineering, Brisbane QLD 4072, Australia, Ph.: (61 7) 3365 4163, Fax: (61 7) 3365 4599, E-mail: h.chanson@uq.edu.au
([3]) Lecturer, Université de Bordeaux, I2M, Laboratoire TREFLE, 16 avenue Pey-Berland, Pessac, France, CNRS UMR 5295, 33607 Pessac, France

Abstract:
A detailed field study was carried out on a tidal bore to document the turbulent processes and sediment entrainment which occurred. The measured bore, within the Arcins Channel of the Garonne River (France), was undular in nature and was followed by well-defined secondary wave motion. Due to the local river geometry a collision between the Arcins channel tidal bore and the bore which formed within the main Garonne River channel was observed about 800 m upstream of the sampling site. This bore collision generated a transient standing wave with a black water mixing zone. Following this collision the bore from the main Garonne River channel propagated ‘backward’ to the downstream end of the Arcins channel. Velocity measurements with a fine temporal resolution were complemented by measurements of the sediment concentration and river level. The instantaneous velocity data indicated large and rapid fluctuations of all velocity components during the tidal bore. Large Reynolds shear stresses were observed during and after the tidal bore passage, including during the 'backward' bore propagation. Large suspended sediment concentration estimates were recorded and the suspended sediment flux data showed some substantial sediment motion, consistent with the murky appearance of the flood tide waters.

Keywords: Tidal bore, Garonne River, Sediment processes, Field observations, Bore collision.

INTRODUCTION

A tidal bore is a hydraulic jump in translation propagating upstream in an estuarine zone, when the tidal flow turns to rising (TRICKER 1965, PEREGRINE 1966, LIGGETT 1994). It is a rapidly-varied unsteady open channel flow generated by the relatively rapid rise in water elevation during the early flood tide, when the tidal range exceeds 4.5 m to 6 m and the funnel shape of both river mouth and lower estuarine zone amplifies the tidal wave (LIGHTHILL 1978, CHANSON 2011a). Figure 1 illustrates tidal bores in China and France, and pertinent accounts include MOORE (1888) and MALANDAIN (1988). Figure 1A shows the undular bore of the Dordogne River (France), which joins the Garonne River downstream off the City of Bordeaux. Figure 1B presents a rare sight of tidal bore crossing in the Qiantang River (China), illustrating the impact of bore crossing on sediment processes.

There has been relatively little investigation to date of the impact on tidal bores on sedimentary processes. Laboratory studies of tidal bores carried out to date have been conducted without suspended sediments, however recent results highlight their importance to erosional processes (MACDONALD et al. 2009, CHANSON 2011b, KHEZRI and CHANSON 2012a). One study on sediment scour used clear-water with a live bed to study the scour inception process (KHEZRI and CHANSON 2012b). Data from field studies have demonstrated the massive impact of tidal bores on sedimentary processes, e.g. suspended sediment transport, bed load, scour and erosion (BARTSCH-WINKLER et al. 1985, FAAS 1995, CHANSON et al. 2011). However, it is challenging to compare data from these different studies due to the differences in hydrodynamic conditions and sediment characteristics (Table 1). Altogether recent findings suggest that (a) the passage of tidal bore is associated with intense sediment scouring and suspension of bed materials (GREB and ARCHER 2007, KHEZRI and CHANSON 2015), (b) the tidal bore advance may contribute to channel shifting in flat and wide bays (CHANSON 2011a), and (c) the very early flood flow may be characterised by very high suspended sediment concentrations (CHANSON et al. 2011, FURGEROT et al. 2013, FAN et al. 2014). Field data exhibited on the other hand different results and trends depending upon the nature of sediment materials (cohesive, non-cohesive, mixture), the site location (e.g. river mouth, inland), site topography (shallow-water bay, constrained river bed), tidal conditions (spring, neap tides) and fluvial discharge (drought, flood).

KEEVIL, C.E., CHANSON, H., and REUNGOAT, D. (2015)." Fluid Flow and Sediment Entrainment in the Garonne River Bore and Tidal Bore Collision." *Earth Surface Processes and Landforms*, Vol. 40, No. 12, pp. 1574-1586 (DOI: 10.1002/esp.3735) (ISSN 0197-9337).

The collision and crossing of tidal bores have been observed in a small number of river systems, where the flow of the incoming flood tide has been split. In Hangzhou Bay (China), the Qiantang River bore develops in two distinct channels: the northern and southern channels. When these channels merge, the previously separate bores cross at a near right angle with spectacular splashing and mixing (Fig. 1B). At the intersection of the two bores, a very turbulent wake region is seen in which the water surface is nearly black, suggesting some intense sediment upwelling in the water column. In shallow water bays, a tidal bore may propagate at different speeds in the braided channels, leading occasionally to some tidal bore collision (e.g. Bay of Mont Saint Michel, France; Kent River estuary, UK). ROWBOTHAM (1983) described the bore of the River Severn advancing at different speeds when split into two channels at Gloucester: "*at the upper end of Alney Island*"; "*the western bore [...] split with much confusion*"; "*part runs down the East Channel and may go as far as the one time Globe Inn at Sandhurst before meeting its tardy brother face to face. After a swirling struggle for supremacy the upward tide inevitably wins*" (ROWBOTHAM 1983, pp. 21-22). There are anecdotal mentions of frontal collision of tidal bores, in the River Trent (UK) and Garonne River (France) (REUNGOAT et al. 2014a). On 6 November 2013, several surfers riding the Petitcodiac River tidal bore (Moncton, Canada) experienced a bore collision, allegedly linked with an upstream reservoir release travelling downstream and colliding head-on with the natural tidal bore (CBC News 2013). The surfers were pushed back over nearly 300 m by the colliding bore: "*During a 10-minute period, the three surfers were caught in a series of whirling currents provoked by the collision of the super bore and the opposing currents* [...]; *After some time they managed to break free and make it to shore safe and sound*". The collision of undular bores was analysed theoretically by BESTEHORN and TYVAND (2009). The phenomenon is identical to an undular bore impacting a solid vertical wall when both bores have the same strength (e.g. STOKER 1957, RAMSDEN 1996), but the development of BESTEHORN and TYVAND (2009) was expanded to bores of different strengths.

Field measurements of tidal bores are currently very limited, although there have been a few studies published to date (Table 1). Table 1 summarises a number of key field studies, highlighting the diversity in instrumentation and flow conditions. Herein new field measurements were conducted on the Garonne River bore (France). Velocity and sediment properties were recorded prior to, during and after passage of the tidal bore in the secondary channel of the Garonne River, and the data were complemented with continuous measurements of water conductivity, temperature and sediment concentration. An unusual feature of the study was the influence of the bore of the main channel of the Garonne River which entered the upstream end of the channel and collided with the main tidal bore. The findings yield a better understanding of the sediment processes in tidal bore-affected rivers, including the effects of tidal bore collision.

METHODS

STUDY SITE AND INSTRUMENTATION

The field study was conducted in the Arcins channel of the Garonne River (France), about 6.5 km south-west of the centre of the City of Bordeaux. The same site was previously used by CHANSON et al. (2011) and REUNGOAT et al. (2014a) (Table 1). The channel is 1.8 km long, 70 m wide and about 1.1 to 2.5 m deep at low tide (Fig. 2 & 3). Figure 2A shows a photograph of the channel. Figure 2B presents a cross-sectional survey conducted on 19 October 2013, in which data are compared with the bathymetric surveys conducted at the same location on 10 September 2010 and 7 June 2012. The survey data indicated some channel siltation since the latest field study. The field measurements were conducted under spring tide conditions on 19 October 2013 afternoon when the tidal range in Bordeaux was 6.09 m. All measurements were made from the hull of a heavy and sturdy pontoon (Fig. 2C) (0º 31' 06.5" W, 44 º 47' 58.6" N). Figure 3 presents a plan view map of the site.

A D&A Instrument^{TM} OBS-5+ (Serial No S5153, Firmware v1.20) unit recorded the suspended sediment concentration about 0.55 m below the water surface. The optical backscatter (OBS) system was sampled at 25 Hz, with the data returned every 10 s at 25 Hz for 5 s. The water temperature, conductivity and pH were recorded about 0.2 m below the water surface. The water temperature was measured manually with a thermometer (Ebro Electronic^{TM} TT100 Type T) as well as with a conductivity, temperature and depth (CTD) self-logging system Model SBE37-SMP (Serial No 3980, Firmware v2.6) sampling at 0.2 Hz. The water conductivity was recorded also with the CTD unit at 0.2 Hz, as well as with a conductivity meter Consort^{TM} C931. The pH was sampled manually with a waterproof pH meter. The instantaneous velocity components were measured with a Nortek^{TM} ADV Vectrino+ (10 MHz, serial number VNO1356), mounted next to the OBS. The acoustic Doppler velocimeter (ADV) system was equipped with a down-looking head

(ADV field). The velocity range was 2.5 m/s, the ADV was set up with a transmit length of 0.3 mm and a sampling volume of 1.5 mm height, and the sampling rate was 200 Hz. The ADV data underwent a post-processing procedure to eliminate any erroneous or corrupted data from the data sets (REUNGOAT et al. 2014b). The percentage of good samples was superior to 82% for the entire data set.
The channel cross-section was surveyed with a Theodolite n"64585 DGT10 CST/berger™. Further observations were recorded with digital single lens reflex (dSLR) cameras and high-definition (HD) digital video cameras.

CHARACTERISATION OF SEDIMENT MATERIALS

Some Garonne River bed material was collected at low tide on 17, 19 and 20 October 2013 afternoons next to the low tide water line on the eastern bank. The soil samples consisted of fine mud and silt materials. Their granulometry was measured with a Malvern™ laser Mastersizer 2000 equipped with a Hydro™ 3000SM dispersion unit for wet samples. The bed sediment samples were mixed mechanically, the granulometry was performed fifteen times with six different data analyses and the results were averaged. The differences between all the runs were negligible.
The rheological properties of mud samples were tested with a Malvern™ Kinexus Pro (Serial MAL1031375) rheometer equipped with a plane-cone (∅ = 40 mm, cone angle: 4°). The gap truncation (150 μm) was selected to be more than ten times the mean particle size. The tests were performed under controlled strain rate at a constant temperature (25 C). Between the sample collection and the tests, the mud was left to consolidate for four days. Prior to each rheological test, a small mud sample was placed carefully between the plate and cone. The specimen was then subjected to a controlled strain rate loading and unloading between 0.01 s^{-1} and 1,000 s^{-1} with a continuous ramp (two minutes ramp time).
The calibration of the ADV and OBS units was accomplished by measuring the ADV and OBS signal amplitudes of known, artificially produced concentrations of material obtained from the bed, diluted in tap water and thoroughly mixed. Tap water was selected for simplicity since previous studies showed that the solution (distilled water, tap water, estuarine water) had little effect on the calibration curve of an ADV (CHANSON et al. 2008, REUNGOAT et al. 2014a). Herein two series of experiments were conducted. During the first series, the laboratory experiments were performed with the Nortek™ ADV Vectrino+ system and OBS-5+ unit using the same settings as for the field measurements on 19 October 2013. For each test, a known mass of wet sediment (density: 1.341) was introduced in a water tank which was continuously stirred with a paint mixer. The mass of wet sediment was measured with a Mettler™ Type PM200 (Serial 86.1.06.627.9.2) balance. The mass concentration was deduced from the measured mass of wet sediment and the measured water tank volume. The average ADV backscatter amplitude measurements represented the average signal strength of the four receivers, and it was measured in counts. The second series of experiments were conducted with the OBS-5+ unit only and each run lasted five minutes. The mass of wet sediment was recorded with an Adams™ PGW753i scale with a precision of 0.001 g. During all the tests, the suspended sediment concentrations (SSCs) ranged from less than 0.01 kg/m^3 to more than 60 kg/m^3.
In addition, a number of water samples were also collected on 19 October 2013 at 16:45 (prior to the arrival of the bore) and 17:45 (during the flood tide) about 0.2 m below the water surface. The water samples were dried in an oven, set at 41 C, to measure the mass of dry sediments for each sample.

SEDIMENT CHARACTERISTICS

The relative density of wet sediment samples was **s** = 1.341-1.41 (Table 2), corresponding to a sample porosity of 0.78-0.75 with a density of dry sediments of 2.65, as checked by drying a number of samples. The particle size distribution data presented close results, irrespective of the collection dates and locations. The median particle size was 15 μm corresponding to some silty material (GRAF 1971, JULIEN 1995) and the sorting coefficient $\sqrt{d_{90} / d_{10}}$ was about 3.7 (Table 2). The bed material was a cohesive mud mixture. The results are compared with previous data at the same site in Table 2. The properties of the Garonne River sediments were similar irrespective of the collection date over the four years period.
Rheometry tests provided some information on the relationship between shear stress and shear rate of the bed material, during the loading and unloading phases of small mud quantities. The data showed some difference between the loading and unloading phases, typical of some form of material thixotropy, the magnitude of shear stress during the unloading phase being consistently smaller than during the loading for a given shear rate (REUNGOAT et al. 2014b). The rheometer data were used to estimate an apparent yield stress τ_c and

effective viscosity μ of the sediment material. Although a complete characterization of a thixotropic material would require the determination of all parameters of a thixotropic model, a rapid, more approximate characterisation of the material was used. The apparent yield stress and effective viscosity were estimated by fitting the rheometry data with a Herschel-Bulkley model, during the unloading phase to be consistent with earlier thixotropic material experiments (COUSSOT 1997, ROUSSEL et al. 2004, CHANSON et al. 2006):

$$\tau = \tau_c + \mu \times \left(\frac{\partial V}{\partial y} \right)^m \quad (1)$$

where τ is the shear stress, $\partial V/\partial y$ is the shear rate and the exponent m satisfies $0 < m \leq 1$ (HUANG and GARCIA 1998, WILSON and BURGESS 1998). A comparison between experimental data and Equation (1) yielded results in terms of the yield stress, effective viscosity and exponent m listed in Table 2. On average, the apparent viscosity was 4.5 Pa.s, the yield stress was about 5.9 Pa and m ~ 0.228 for the sediment sample collected on 19 October 2013 at low tide. The repeatability of the rheometry tests was checked by testing identically different samples; the results were very close as seen in Table 2. Present findings of τ_c = 5 to 6 Pa were comparable to previous investigations at the same site (CHANSON et al. 2011, REUNGOAT et al. 2014a, Table 2), although the data were quantitatively consistent with the qualitative observation of softer sediment samples.

The relationships between backscatter amplitude of ADV and OBS units and suspended sediment concentrations (SSCs) were tested systematically in two laboratories (University of Bordeaux and University of Leeds), for SSCs between 0 and 100 kg/m^3. The experimental results are summarised in Figure 4. The data showed similar qualitative trends for the OBS and ADV units: the data indicated a monotonic increase in suspended sediment concentration with increasing backscatter amplitude for SSC less than 2 to 10 kg/m^3. For larger SSCs (i.e. SSC > 10 kg/m^3), the experimental results showed a decreasing backscatter amplitude with increasing SSC, although it was more significant with the OBS data. The general trends were consistent with a number of studies, including with cohesive sediment materials (DOWNING et al. 1995, HA et al. 2009, GUERRERO et al. 2011, CHANSON et al. 2011, BROWN and CHANSON 2012). Sediment-laden water samples were collected at Arcins in the Garonne River on 19 October 2013 before and after the tidal bore and analysed subsequently in both laboratories. The samples indicated a low suspended sediment concentration prior to the tidal bore, with SSC about 2 kg/m^3 at 16:59; a higher SSC, about 9.5 kg/m^3, was seen at 17:45, about 40 minutes after the bore passage. The sediment-laden water sample data analyses were compared with the calibration data of the ADV and OBS units in Figure 4 (errors bars added for completeness). The results exhibited a reasonable agreement between the measured SSCs and ADV and OBS backscatter readings for both water samples, implying that the backscatter amplitude outputs may be used as a surrogate of SSC with the proper selection of some calibration curve. All the field observations indicated that the suspended sediment concentrations (SSCs) were very low prior the tidal bore, while much larger sediment concentration levels were observed during and after the passage of the tidal bore. As a result, the SSC estimates were calculated using the following OBS calibration curve for SSC < 6 kg/m^3:

$$SSC = 0.235 \times 1.0039^{NTU} \times NTU^{0.147} \quad \text{SSC < 6 kg/m}^3 \text{ (OBS)} \quad (2)$$

where the OBS backscatter amplitude (NTU) is in nephelometric turbidity units, and the suspended sediment concentration (SSC) is in kg/m^3. During and after the passage of the tidal bore, the SSCs were significantly larger and the OBS backscatter amplitude was attenuated by the heavily sediment-laden flow. The suspended sediment estimates were deduced from the OBS calibration data for SSC > 10 kg/m^3:

$$SSC = 59.26 \times e^{-0.00226 \times NTU} \quad \text{SSC > 10 kg/m}^3 \text{ (OBS)} \quad (3)$$

Equations (2) and (3) were applied to the field data set before and after the tidal bore passage respectively. The results are presented and discussed below.

The velocity and SSC data were used to calculate the instantaneous suspended sediment flux per unit area $q_s = SSC \times V_x$ where q_s and V_x are positive in the downstream direction, SSC is in kg/m^3, and the sediment flux per unit area q_s is in kg/m^2/s. Herein the suspended sediment concentration (SSC) was estimated from the median OBS data and the longitudinal velocity was averaged over 5 s.

RESULTS

FLOW PATTERNS AND OBSERVATIONS

The tidal bore formed at the downstream end of the Arcins channel and extended across the entire channel width. The bore shape evolved in response to the local bathymetry as the bore propagated upstream. It was

undular at the sampling location (Fig. 2A & 5) and the bore front was well highlighted by two experienced surfers riding ahead of the first wave crest. The free-surface elevation rose very rapidly by 0.3 m in the first 10-15 seconds (Fig. 6). For the next 60 s, the water elevation rose further by 1.1 m. The bore passage was immediately followed by a series of secondary waves lasting for a couple of minutes, with a wave period of about 1 s. During the field study, the water temperature varied from 18.7 C to 17.9 C and the water conductivity ranged from 25 mS/cm to 31 mS/cm depending upon the instrument, although each sensor data varied within only 2 mS/cm. The pH data ranged from 7.6 down to 7 with a monotonic decrease in pH during the afternoon. Importantly the present observations indicated an absence of a saline front, temperature front or pH front, associated with the tidal bore passage in the Arcins channel.

Whilst the tidal bore advanced in the Arcins channel, another bore progressed into the main channel of the Garonne River (Fig. 3). During the current field study, the bore of the main channel entered into the Arcins channel at its upstream end, forming a marked bore propagating northwards (i.e. downstream) against the flood tide (Fig. 5C). As the Arcins channel tidal bore approached the upstream end of the channel, it collided with the 'backward' bore of the main channel about 3 min. 53 s after it passed the sampling site (Fig. 5C). Figure 3 presents a plan view sequence of the process, with the sketch No. 3 corresponding to a situation shortly prior to the bore collision seen in Figure 5C. The tidal bore collision was experienced first hand by the two surfers seen in Figure 5C: when the two bores collided, one surfer kneeled on his board while the second surfer remained standing but moved closer to the right bank (i.e. eastern bank). They described the bore collision as a very turbulent standing wave, associated with a rapid water level rise (REUNGOAT et al. 2014b). While both surfers continued to surf the bore front southwards, their absolute speed dropped sharply as the standing wave formed and was almost stationary. BESTEHORN and TYVAND (2009) provided a mathematical description for the formation of such a standing wave, after the collision of two undular bores. The bore collision generated a very dark black water mixing zone, evidence of massive sediment convection to the free-surface (Fig. 5C). The collision was an unique experience for these two experienced tidal bore surfers.

After collision, the tidal bore of the Garonne River main channel continued to propagate downstream against the flood tide in the Arcins channel, with wave breaking seen next to the left and right banks (Fig. 5D). In Figure 3 Right, the sketch No. 4 corresponds to the situation seen in Figure 5D. The celerity of this 'backward' bore was between 1.5 to 2.5 m/s, compared to the celerity of the Arcins channel tidal bore of 4.3 m/s. The 'backward' bore reached the sampling station 9 min 32 s after the Arcins channel bore passed the ADV unit and continued until it reached the downstream end of the Arcins channel, where it vanished as the channel expanded. At the sampling station, the passage of the 'backward' bore was felt by the authors, with a sudden flow deceleration, associated with a northward surface flow motion next to the right bank and very strong turbulence next to the pontoon.

VELOCITY MEASUREMENTS

The instantaneous velocity components were measured prior to, during and after the tidal bore. The entire data set is reported in Figure 6, with the longitudinal velocity component V_x positive downstream. The time-variations of the water depth are included as well as the surface velocity data recorded using floating debris and stop watches on the channel centreline. Both the centreline surface velocity and ADV velocity data were very close prior to the bore passage: at the end of ebb tide, the current velocity was about +0.1 m/s, immediately prior to the bore passage. The tidal bore passage (t = 61,518 s) induced a marked effect on the longitudinal velocity (Fig. 6). The current reversed its direction and the longitudinal velocity component was negative, between -0.8 and -1.2 m/s, at the ADV sampling location. For comparison, the surface velocity on the channel centreline ranged between -1.2 and -2.6 m/s. The ADV sampling volume was located about 3 m from the right bank slope at low tide, and the slower ADV velocity data might reflect the effect of river bank boundary proximity. The passage of the bore was associated with large fluctuations of all three velocity components, including during the early ebb tide (Fig. 6). About 570 s after the bore passage, the 'backward' bore of the main Garonne River channel reached the ADV unit. Its effect was felt with a drop in water elevation as well as a slower upstream flow motion, illustrated in Figure 6. (In Figure 6, the vertical dashed lines show the arrival of the tidal bore and 'backward' bore.) The flow deceleration experienced during the passage of the 'backward' bore may be predicted theoretically in the case of colliding bores, once the smaller 'backward' bore continue downstream. Large fluctuations of all velocity components were recorded during the 'backward' bore event (62,100 < t < 62,300 s, Fig. 6). Altogether the propagation of the 'backward' bore induced some intense turbulent mixing, in addition to the strong surface mixing observed visually next to the

right and left banks.

TURBULENT REYNOLDS STRESS MEASUREMENTS

A turbulent Reynolds stress is proportional to the product of two velocity fluctuations, where the turbulent velocity fluctuation v is the deviation of the instantaneous velocity from an average $\overline{V}$. Herein $\overline{V}$ was the low-pass filtered velocity component, or variable interval time average VITA (PIQUET 1999, CHANSON and DOCHERTY 2012). The cut-off frequency F_{cutoff} was derived based upon a sensitivity analysis conducted between an upper limit of the filtered signal (herein 100 Hz, the Nyquist frequency) and a lower limit corresponding to a period of about 0.96 s of the bore undulations. The results yielded an optimum threshold of F_{cutoff} = 2 Hz. The filtering was applied to all velocity components and the turbulent Reynolds stresses were calculated from the high-pass filtered signals. Typical results are presented in Figure 7.

The field observations showed large turbulent shear stresses, and large and rapid fluctuations in shear stresses during and after the tidal bore, for all Reynolds stress tensor components. The data highlighted also large magnitudes of shear stresses at about the time of passage of the 'backward' bore (Fig. 7, t = 62,149 s). The turbulent shear stresses were significantly larger after the tidal bore passage: the mean normal stresses were four to sixteen times larger after the tidal bore passage than before, the standard deviations of all stress components were two to ten times larger after the tidal bore passage, and the maximum instantaneous Reynolds shear stresses were two to three times larger after the tidal bore. Herein maximum instantaneous shear stress amplitudes of up to 94 Pa were recorded, shortly (a few minutes) after the passage of the 'backward' bore. The data implied that the bore has the potential to scour the natural bed, with instantaneous stresses significantly larger than the material yield stress τ_c which is related to the minimum boundary shear stress required to erode and re-suspend cohesive sediments (OTSUBO and MURAOKO 1988, VAN KESSEL and BLOM 1998). The tidal bore most likely scoured the channel bed and advected into suspension the bed material and carried the suspended sediments, behind the bore front during the early flood tide. This process applied to a significant length of the estuarine section of the Garonne River and would mobilise an enormous amount of sediments.

SUSPENDED SEDIMENT PROCESSES

The time-variations of suspended sediment concentration (SSC) estimates were deduced from the OBS data and are presented in Figure 8A. Note that the present data were median data calculated over 5 s. The water depth data are shown also in Figure 8A as well as the sediment concentrations of water samples tested in laboratory. The data showed some low SSC, 2.6 kg/m^3 on average, at the end of the ebb tide and the findings were close to the laboratory data (SSC = 2.12 kg/m^3). The passage of the tidal bore was associated with large fluctuations in SSC estimates. The 'backward' bore event induced even larger SSCs and SSC fluctuations, consistent with the large turbulent stress levels generated during the 'backward' bore passage which delayed the deposit of sediments (Fig. 8A). The finding was consistent with both the visual observations and the turbulent Reynolds stress data set. During the later flood tide, the SSC estimates tended to 13-15 kg/m^3 on average.

The instantaneous suspended sediment flux per unit area q_s data are presented in Figure 8B. The sediment flux data indicated a downstream positive mass flux during the end of ebb tide. On average, the suspended sediment flux per unit area was 0.5 kg/m^2/s prior to the tidal bore. The tidal bore passage was characterised by a sudden flow reversal and the suspended sediment flux was negative during the flood tide. The sediment flux data q_s showed some large fluctuations. Shortly after the bore passage and during the 'backward' bore event, the sediment flux per unit reached very large mean negative values up to -73 kg/m^2/s (Fig. 8B). About 45 minutes after the tidal bore, the sediment flux was -15 kg/m^2/s on average.

The sediment flux data were integrated with respect to time to yield the net sediment mass transfer per unit area during a given period. Prior the tidal bore (60,800 < t < 61,511 s), the net sediment mass transfer per unit area was +742 kg/m^2 for 12 minutes of data. Immediately following the tidal bore passage, the net sediment mass transfer equalled -39,970 kg/m^2 for 17 minutes (61,535 < t < 62,574 s). Towards the end of the study, the net sediment mass transfer equalled -32,000 kg/m^2 for 36 minutes (63,378 < t < 65,530 s). The data set highlighted the drastic impact of the 'backward' bore, not previously observed in earlier field studies. During the passage of the tidal bore and 'backward' bore event, the net sediment flux amplitude was about 38 times larger in magnitude than prior to the tidal bore, and 2.5 times larger than later during the flood tide.

KEEVIL, C.E., CHANSON, H., and REUNGOAT, D. (2015)." Fluid Flow and Sediment Entrainment in the Garonne River Bore and Tidal Bore Collision." *Earth Surface Processes and Landforms*, Vol. 40, No. 12, pp. 1574-1586 (DOI: 10.1002/esp.3735) (ISSN 0197-9337).

DISCUSSION

The downstream propagation of the 'backward' bore was a new feature which was not observed during previous field studies. It was believed to be linked with the recent siltation of the Arcins channel, which delayed the propagation of the tidal bore in the Arcins channel, since the bore celerity is proportional to the initial water depth:

$$U + V_1 \propto \sqrt{g \times \frac{A_1}{B_1}} \times \sqrt{1+\varepsilon} \quad (4)$$

where ε is a term of second order (TRICKER 1965, LIGHTHILL 1978). The siltation of the Arcins channel might occur like the cutoff of secondary channels in meandering rivers (DOEGLAS 1962, PARKER et al. 2011). The build-up of a low natural bar of hard materials was observed at the upstream end of the Arcins channel in mid-2013. It is conceivable that the major flood of the Garonne River in 2012 scoured the main channel, west of Arcins Island, reducing the ebb flow in the Arcins channel during low waters.

In October 2013, a feature of the river channel was a series of longitudinal rills along the right bank at low tide for most of the length of the Arcins channel. Figure 5A illustrates such rills next to the sampling station (Fig. 5A, right with white arrow). The longitudinal forms looked like elongated, two dimensional bed forms somehow similar to those reported by CARLING et al. (2009) in the lower estuary of River Severn, although with some key differences. The raised sections of River Severn were wider, with broader intermediary runnels and much longer runs. It is suggested that the bed form formation at Arcins was closely linked with some form of wash effect from the changing tide, the existence of the 'backward' bore flow and its induced turbulent mixing. Visual observations indicated that the elevation of the bed forms corresponded to the flooding induced by the 'backward' bore. Alternatively the longitudinal bed forms at Arcins could be possibly older drag marks induced by some large debris and preserved across several tides. At this stage, no definite conclusion can be drawn.

The present field data highlighted a significant suspended sediment load during the tidal bore, including during the 'backward' bore event. Table 3 regroups the results in terms of the mean suspended sediment concentration and average suspended sediment flux per unit area during the early flood tide. Two data sets are shown for the distinctively different periods: (a) during the tidal bore event and 'backward' bore, and (b) after the 'backward' bore. The present data were compared with the earlier suspended sediment load data in the Garonne River tidal bores in 2010 and 2012 (CHANSON et al. 2011, REUNGOAT et al. 2014a). Any comparison between the present findings and earlier data in the Arcins channel must be considered with care, because of the difference in instrumentation and type of data (instantaneous vs average) (Table 1). Altogether the present data showed large suspended sediment fluxes per unit area and SSCs observed during the Garonne River tidal bore and early flood tide. To date a few studies have highlighted the intense sediment mixing and upstream advection of suspended matters during the passage of a tidal bore (CHEN et al. 1990, GREB and ARCHER 2007, CHANSON et al. 2011, FURGEROT et al. 2013, REUNGOAT et al. 2014a). The present data set supported the same trend, and they showed further the drastic impact of tidal collision in terms of sediment processes.

The sediment deposit samples were predominantly silty material that exhibited a non-Newtonian behaviour under rheological testing (see above). The rheological properties of the sediment deposits were directly relevant to the inception of sediment materials and properties of the dilute suspension. The apparent yield stress of the mud provided some quantitative information on the critical shear stress for sediment erosion. Previous studies indicated that the critical shear stress for mud erosion and sediment re-suspension is close to and slightly lower than the yield stress (OTSUBO and MURAOKO 1988, VAN KESSEL and BLOM 1998, HOBSON 2008, SANCHEZ and LEVACHER 2008, JACOBS et al. 2011). Once the fluid shear stress exceeds the local strength of the bed, surface erosion occurs initially, in the form of stripping and aggregate fragmentation (POUV et al. 2014). This is followed after some time by mass erosion, occurring rapidly (AMOS et al. 1992, WINTERWERP and VAN KESTERE 2004). In laboratory, POUV et al. (2014) observed bulk erosion about 7 to 40 minutes after the experiment start depending upon the test conditions. The same erosion processes were likely observed in the Arcins channel. It is believed that the passage of the tidal bore induced a drastic increased in fluid shear stress that induced immediately some surface erosion of the bed material, followed by delayed mass erosion. The latter would be consistent with the present observations of sediment upwelling and sediment flocs bursting at the free-surface for next two hours, similar observations by CHANSON et al. (2011), as well as with the observations of fold-shaped and 'tobacco·pouch'-shaped scour forms, cusps and depressions observed in France and Canada (TESSIER and

TERWINDT 1994, FAAS 1995).
Once the sediment bed material was eroded and entrained by the bore, the present rheological data implied that, at high suspended sediment concentrations, the flood tide waters might exhibit some non-Newtonian characteristics, and their behaviour cannot be predicted accurately without a detailed rheological characterisation of the sediment materials (WANG et al. 1994, ANTOINE et al. 1995, COUSSOT 1997,2005, BROWN and CHANSON 2012). Using dilute suspensions of bentonite, CHANSON et al. (2006) showed a non-Newtonian thixotropic flow behaviour using both dam break wave experiment and rheometry data, while COUSSOT and OVARLEZ (2010) demonstrated the non-Newtonian thixotropic behaviour of dilute suspensions of bentonite using direct magnetic resonance imaging (MRI). These results suggested a non-Newtonian behaviour of dilute suspensions for mass concentrations as low as 1%. During the present field investigation, SSC estimates between 10 kg/m^3 and 60 kg/m^3 were observed during the tidal bore and early flood tide (Figure 8A), corresponding to mass concentrations between 1 and 6%. The present SSC estimates, together with the sediment rheological data, implied that the early flood tide flow with high suspended sediment concentrations might exhibit some form of non-Newtonian flow behaviour. This has never been taken into account in conceptual and hydrodynamic models.

CONCLUSION

A detailed field study was conducted in the Garonne River at Arcins (France) to characterise the turbulent and sedimentary processes of the tidal bore. Key features of the investigation included the fine temporal resolution with a 200 Hz velocity sampling rate, the complementary nature of the instruments (ADV, OBS, CTD) and a comprehensive characterisation of the sediment properties including granulometry and rheology. The sediment samples were predominantly silty material with a median particle size about 15 μm and they exhibited a non-Newtonian thixotropic behaviour under rheological testing.
The tidal bore was undular and the undular front was followed by well-defined whelps with wave period about 1 s. A most unusual feature was the collision between the Arcins channel tidal bore and the bore of the Garonne River main channel. The bore collision occurred close to the upstream end of the Arcins channel about 800 m from the sampling site. It was well-documented by two surfers and a number of photographs. The collision of the bores generated a transient standing wave with a dark blackwater mixing zone. The Garonne River main channel bore propagated 'backward' along the Arcins channel with some breaking next to the river bank. Its effects were felt at the sampling site with a temporary lowering of the water surface and flow deceleration.
The instantaneous velocity data indicated large Reynolds shear stresses observed during and after the tidal bore, including during the 'backward' bore propagation. Large SSC estimates were observed in the tidal bore and early flood tide. Based upon the rheological characteristics of bed material, it is proposed that the bore passage induced immediately some surface erosion followed by delayed bulk erosion. During the tidal bore passage, the 'backward' bore event, and the early flood tide, the suspended sediment flux data showed some substantial sediment suspension amplitudes consistent with the murky appearance of flood tide waters.
The collision of tidal bores in the Arcins channel was a most unusual occurrence. It is proposed that this phenomenon was caused by the relatively recent siltation of the Arcins channel, delaying the propagation of the tidal bore in the silted channel and allowing the main channel bore to enter and develop at the upstream end of the Arcins channel. All the quantitative data, sampled at 800 m north of the collision site, indicated a massive impact of the bore collision on the entire Arcins channel system.

ACKNOWLEDGEMENTS

The authors thank Dr Frédérique LARRARTE (IFSTTAR Nantes) and Professor Michael BESTEHORN (Brandenburg University of Technology) for their initial comments. They acknowledge the helpful inputs of Professor Dan PARSONS (University of Hull), Professor Pierre LUBIN (University of Bordeaux), Dr Eric JONES (Proudman Oceanographic Laboratory) and the journal reviewers. The authors acknowledge the assistance of Patrice BENGHIATI and the permission to access and use the pontoon in the Bras d'Arcins. They thank all the people who participated to the field works, and without whom the study could not have been conducted, and the SEFDL at the University of Leeds for the loan of equipment. They also thank Frédéric DANEY (Bordeaux, France), and Daniel LEBLANC (Moncton, Canada) for a number of useful discussions and information. The authors acknowledge the financial assistance of the Agence Nationale de la Recherche (Projet MASCARET 10-BLAN-0911-01).

KEEVIL, C.E., CHANSON, H., and REUNGOAT, D. (2015)." Fluid Flow and Sediment Entrainment in the Garonne River Bore and Tidal Bore Collision." *Earth Surface Processes and Landforms*, Vol. 40, No. 12, pp. 1574-1586 (DOI: 10.1002/esp.3735) (ISSN 0197-9337).

REFERENCES

AMOS, C.L., DABORN, G.R., CHRISTIAN, H.A., ATKINSON, A., and ROBERTSON, A. (1992)." In situ erosion measurements on fine grained sediments from the Bay of Fundy." Marine Geology, Vol. 108, pp. 175–96 (DOI: 10.1016/0025-3227(92)90171-D).

ANTOINE, P., GIRAUD, A., MEUNIER,M., and VAN ASCH, T. (1995). "Geological and geotechnical properties of the ‘‘Terres Noires’’ in southeastern France: Weathering, erosion, solid transport and instability." *Engineering Geology*, Vol. 40, pp. 223–234.

BARTSCH-WINKLER, S., EMANUEL, R.P., and WINKLER, G.R. (1985). "Reconnaissance hydrology and suspended sediment analysis, Turnagain Arm estuary, upper Cook Inlet." in "The United States Geological Survey in Alaska; accomplishments during 1984" *U.S. Geological Survey Circular 967*, S. BARTSCH-WINKLER Editor, p. 49-51.

BESTEHORN, M., and TYVAND, P.A. (2009). "Merging and Colliding Bores." *Physics of Fluids*, Vol. 21, Paper 042107, 11 pages (DOI: 10.1063/1.3115909).

BROWN, R., and CHANSON, H. (2012). "Suspended Sediment Properties and Suspended Sediment Flux Estimates in an Urban Environment during a Major Flood Event." *Water Resources Research*, AGU, Vol. 48, Paper W11523, 15 pages (DOI: 10.1029/2012WR012381).

CARLING, P.A., WILLIAMS, J.J., CROUDACE, I.W., and AMOS, C.L. (2009). "Formation of Mud Ridge and Runnels in the Intertidal Zone of the Severn Estuary, UK." *Continental Shelf Research*, Vol. 29, pp. 1913-1926 (DOI: 10.1016/j.csr.2008.12.009).

CBC News (2013). "5 super bore surfers hit by surprise wave in Moncton." {http://www.cbc.ca/news/canada/new-brunswick/5-super-bore-surfers-hit-by-surprise-wave-in-moncton-1.2418096} (Webpage accessed on 2 Dec. 2013).

CHANSON, H. (2011a). "Tidal Bores, Aegir, Eagre, Mascaret, Pororoca: Theory and Observations." *World Scientific*, Singapore, 220 pages (ISBN 9789814335416).

CHANSON, H. (2011b). "Turbulent Shear Stresses in Hydraulic Jumps and Decelerating Surges: An Experimental Study." *Earth Surface Processes and Landforms*, Vol. 36, No. 2, pp. 180-189 & 2 videos (DOI: 10.1002/esp.2031).

CHANSON, H., and DOCHERTY, N.J. (2012). "Turbulent Velocity Measurements in Open Channel Bores." *European Journal of Mechanics B/Fluids*, Vol. 32, pp. 52-58 (DOI 10.1016/j.euromechflu.2011.10.001).

CHANSON, H., JARNY, S., and COUSSOT, P. (2006). "Dam Break Wave of Thixotropic Fluid." *Journal of Hydraulic Engineering*, ASCE, Vol. 132, No. 3, pp. 280-293 (DOI: 10.1061/(ASCE)0733-9429(2006)132:3(280)).

CHANSON, H., REUNGOAT, D., SIMON, B., and LUBIN, P. (2011). "High-Frequency Turbulence and Suspended Sediment Concentration Measurements in the Garonne River Tidal Bore." *Estuarine Coastal and Shelf Science*, Vol. 95, No. 2-3, pp. 298-306 (DOI 10.1016/j.ecss.2011.09.012).

CHANSON, H., TAKEUCHI, M., and TREVETHAN, M. (2008). "Using Turbidity and Acoustic Backscatter Intensity as Surrogate Measures of Suspended Sediment Concentration in a Small Sub-Tropical Estuary." *Journal of Environmental Management*, Vol. 88, No. 4, Sept., pp. 1406-1416 (DOI: 10.1016/j.jenvman.2007.07.009).

CHEN, Jiyu, LIU, Cangzi, ZHANG, Chongle, and WALKER, H.J. (1990). "Geomorphological Development and Sedimentation in Qiantang Estuary and Hangzhou Bay." *Jl of Coastal Res.*, Vol. 6, No. 3, pp. 559-572.

CHEN, S. (2003). "Tidal Bore in the North Branch of the Changjiang Estuary." *Proc. Intl Conf. on Estuaries & Coasts ICEC-2003*, Hangzhou, China, Nov. 8-11, Intl Research & Training Center on Erosion & Sedimentation Ed., Vol. 1, pp. 233-239.

COUSSOT, P. (1997). "Mudflow Rheology and Dynamics." *IAHR Monograph*, Balkema, The Netherlands.

COUSSOT, P. (2005). "Rheometry of Pastes, Suspensions, and Granular Materials. Applications in Industry and Environment." *John Wiley*, New York, USA, 291 pages.

DOEGLAS, D.J. (1962). "The Structure of Sedimentary Deposits of Braided Rivers." *Sedimentology*, Vol. 1, pp. 167-193.

DOWNING, A., THORNE, P.D., VINCENT, C.E. (1995). "Backscattering from a suspension in the near field of a piston transducer." *Journal of Acoustical Society of America*, Vol. 97, No. 3, pp. 1614-1620.

FAAS, R.W. (1995). "Rheological Constraints on Fine Sediment Distribution and Behavior: The Cornwallis Estuary, Novia Scotia." *Proc. Can. Coastal. Conf.*, Dartmouth, Nova Scotia, pp. 301–314.

KEEVIL, C.E., CHANSON, H., and REUNGOAT, D. (2015)." Fluid Flow and Sediment Entrainment in the Garonne River Bore and Tidal Bore Collision." *Earth Surface Processes and Landforms*, Vol. 40, No. 12, pp. 1574-1586 (DOI: 10.1002/esp.3735) (ISSN 0197-9337).

FAN, D., TU, J., SHANG, S., and CAI, G. (2014). "Characteristics of tidal-bore deposits and facies associations in the Qiantang Estuary, China." *Marine Geology*, Vol. 348, pp. 1-14 (DOI: 10.1016/j.margeo.2013.11.012).

FURGEROT, L., MOUAZE, D., TESSIER, B., PEREZ, L., and HAQUIN, S. (2013). "Suspended Sediment Concentration in Relation to the Passage of a Tidal Bore (Sée River Estuary, Mont Saint Michel, NW France)." *Proc. Coastal Dynamics 2013*, Arcachon, France, 24-28 June, pp. 671-682.

GRAF, W.H. (1971). "Hydraulics of Sediment Transport." *McGraw-Hill*, New York, USA.

GREB, S.F., and ARCHER, A.W. (2007). "Soft-Sediment Deformation Produced by Tides in a Meizoseismic Area, Turnagain Arm, Alaska." *Geology*, Vol. 35, No. 5, pp. 435-438.

GUERRERO, M., SZUPIANY, R.N., and AMSLER, M. (2011). "Comparison of Acoustic Backscattering Techniques for Suspended Sediments Investigation." *Flow Measurement & Instrumentation*, Vol. 22, pp. 392-401.

HA, H.K., HSU, W.Y., MAA, J.P.Y., SHAO, Y.Y., and HOLLAND, C.W. (2009). "Using ADV Backscatter Strength for Measuring Suspended Cohesive Sediment Concentration." *Continental Shelf Research*, Vol. 29, pp. 1310-1316.

HOBSON, P.M. (2008). "Rheologic and Flume Erosion Characteristics of Georgia Sediments from Bridge Foundations." *MSc thesis*, School of Civil and Environmental Engineering, Georgia Institute of Technology, 108 pages.

HUANG, X., and GARCIA, M. (1998). "A Herschel-Bulkley Model for Mud Flow Down a Slope." *Jl of Fluid Mech.*, Vo. 374, pp. 305-333.

JACOBS, W., LE HIR, P., VAN KESTEREN, W., and CANN, P. (2011). "Erosion threshold of sand–mud mixtures." *Continental Shelf Research*, Vol. 31, Supplement, pp. S14–S25 (DOI: 10.1016/j.csr.2010.05.012).

JULIEN, P.Y. (1995). "Erosion and Sedimentation." *Cambridge University Press*, Cambridge, UK, 280 pages.

KHEZRI, N., and CHANSON, H. (2012a). "Undular and Breaking Tidal Bores on Fixed and Movable Gravel Beds." *Journal of Hydraulic Research*, IAHR, Vol. 50, No. 4, pp. 353-363 (DOI: 10.1080/00221686.2012.686200).

KHEZRI, N., and CHANSON, H. (2012b). "Inception of Bed Load Motion beneath a Bore." *Geomorphology*, Vol. 153-154, pp. 39-47 (DOI: 10.1016/j.geomorph.2012.02.006).

KHEZRI, N., and CHANSON, H. (2015). "Turbulent Velocity, Sediment Motion and Particle Trajectories under Breaking Tidal Bores: Simultaneous Physical Measurements." *Environmental Fluid Mechanics*, Vol. 15, No. 3, pp. 633-651 (DOI: 10.1007/s10652-014-9358-z) & (DOI: 10.1007/s10652-014-9360) (ISSN 1567-7419 [Print] 1573-1510 [Online]).

KJERFVE, B., and FERREIRA, H.O. (1993). "Tidal Bores: First Ever Measurements." *Ciência e Cultura (Jl of the Brazilian Assoc. for the Advancement of Science)*, Vol. 45, No. 2, March/April, pp. 135-138.

LEWIS, A.W. (1972). "Field Studies of a Tidal Bore in the River Dee." *M.Sc. thesis*, Marine Science Laboratories, University College of North Wales, Bangor, UK.

LIGGETT, J.A. (1994). "Fluid Mechanics." *McGraw-Hill*, New York, USA.

LIGHTHILL, J. (1978). "Waves in Fluids." *Cambridge University Press*, Cambridge, UK, 504 pages.

MACDONALD, R.G., ALEXANDER, J., BACON, J.C., and COOKER, M.J. (2009). "Flow patterns, sedimentation and deposit architecture under a hydraulic jump on a non-eroding bed: defining hydraulic-jump unit bars." *Sedimentology*, Vol. 60, pp. 1291-1312.

MALANDAIN, J.J. (1988). "La Seine au Temps du Mascaret." ('The Seine River at the Time of the Mascaret.') *Le Chasse-Marée*, No. 34, pp. 30-45 (in French).

MOORE, R.N. (1888). "Report on the Bore of the Tsien-Tang Kiang." *Hydrographic Office*, London.

MOUAZE, D., CHANSON, H., and SIMON, B. (2010). "Field Measurements in the Tidal Bore of the Sélune River in the Bay of Mont Saint Michel (September 2010)." *Hydraulic Model Report No. CH81/10*, School of Civil Engineering, The University of Queensland, Brisbane, Australia, 72 pages (ISBN 9781742720210).

NAVARRE, P. (1995). "Aspects Physiques du Caractère Ondulatoire du Macaret en Dordogne." ('Physical Features of the Undulations of the Dordogne River Tidal Bore.') *D.E.A. thesis*, University of Bordeaux, France, 72 pages (in French).

OTSUBO, K. and MURAOKO, K. (1988). "Critical shear stress of cohesive bottom sediments." *Journal of Hydraulic Engineering*, ASCE, Vol. 114, No. 10, pp. 1241-1256.

KEEVIL, C.E., CHANSON, H., and REUNGOAT, D. (2015)." Fluid Flow and Sediment Entrainment in the Garonne River Bore and Tidal Bore Collision." *Earth Surface Processes and Landforms*, Vol. 40, No. 12, pp. 1574-1586 (DOI: 10.1002/esp.3735) (ISSN 0197-9337).

PARKER, G., SHIMIZU, Y., WILKERSON, G.V., EKE, E.C., ABAD, J.D., LAUER, J.W., PAOLA, C., DIETRICH, W.E., and VOLLER, V.R. (2011). "A New Framework for Modeling the Migration of Meandering Rivers." Earth Surface Processes and Landforms, Vol. 36, pp. 70-86.

PEREGRINE, D.H. (1966). "Calculations of the Development of an Undular Bore." *Jl. Fluid Mech.*, Vol 25, pp.321-330.

PIQUET, J. (1999). "Turbulent Flows. Models and Physics." *Springer*, Berlin, Germany, 761 pages.

POUV, K.S., BESQ, A., GULLOU, S.S., and TOORMAN, E.A. (2014). "On cohesive sediment erosion: A first experimental study of the local processes using transparent model materials." *Advances in Water Resources*, Vol. 72, pp. 71-83.

RAMSDEN, J.D. (1996). "Forces on a Vertical Wall due to Long Waves, Bores and Dry-Bed Surges." *Journal of Waterway, Port, Coastal and Ocean Engineering*, ASCE, Vol. 122, No. 3, pp. 134-141.

REUNGOAT, D., CHANSON, H., and CAPLAIN, B. (2014a). "Sediment Processes and Flow Reversal in the Undular Tidal Bore of the Garonne River (France)." *Environmental Fluid Mechanics*, Vol. 14, No. 3, pp. 591-616 (DOI: 10.1007/s10652-013-9319-y).

REUNGOAT, D., CHANSON, H., and KEEVIL, C. (2014b). "Turbulence, Sedimentary Processes and Tidal Bore Collision in the Arcins channel, Garonne River (October 2013)." *Hydraulic Model Report No. CH94/14*, School of Civil Engineering, The University of Queensland, Brisbane, Australia, 145 pages (ISBN 9781742721033).

ROUSSEL, N., LE ROY, R., and COUSSOT, P. (2004). "Thixotropy Modelling at Local and Macroscopic Scales." *Jl of Non-Newtonian Fluid Mech.*, Vol. 117, No. 2-3, pp. 85-95.

ROWBOTHAM, F. (1983). "The Severn Bore." *David & Charles*, Newton Abbot, UK, 3rd edition, 104 pages.

SANCHEZ, M., and LEVACHER, D. (2008). "Erosion d'une vase de l'estuaire de la Loire sous l'action du courant." ('Erosion of a mud from the Loire estuary by a flow.') *Bull Eng Geol Environ*, Vol. 67, pp. 597–605 (DOI: 10.1007/s10064-008-0159-9).

SIMPSON, J.H., FISHER, N.R., and WILES, P. (2004). "Reynolds Stress and TKE Production in an Estuary with a Tidal Bore." *Estuarine, Coastal and Shelf Science*, Vol. 60, No. 4, pp. 619-627.

STOKER, J.J. (1957). Water Waves. The Mathematical Theory with Applications." *Interscience Publishers*, New York, USA, 567 pages.

TESSIER, B., and TERWINDT, J.H.J. (1994). "An Example of Soft-Sediment Deformations in an intertidal Environment - The Effect of a Tidal Bore". *Comptes-Rendus de l'Académie des Sciences*, Série II, Vol. 319, No. 2, Part 2, pp. 217-233 (in French).

TRICKER, R.A.R. (1965). "Bores, Breakers, Waves and Wakes." *American Elsevier Publ. Co.*, New York, USA.

VAN KESSEL, T, and BLOM, C. (1998). "Rheology of cohesive sediments: comparison between a natural and an artificial mud." Journal of Hydraulic Research, IAHR, Vol. 36, No. 4, pp. 591–612.

WANG, Z.Y., LARSEN, P., and XIANG, W. (1994). "Rheological properties of sediment suspensions and their implications." *Journal of Hydraulic Research*, IAHR, Vol. 32, No. 4, pp. 495–516.

WILSON, S.D.R., and BURGESS, S.L. (1998). "The Steady, Speading Flow of a Rivulet of Mud." *Jl Non-Newtonian Fluid Mech.*, Vol. 79, pp. 77-85.

WINTERWERP, J.C., and VAN KESTEREN, W.G.M. (2004). "Introduction to the Physics of Cohesive Sediment in the Marine Environment." *Elsevier*, Developments in Sedimentology Vol. 56, Editor T. VAN LOON, Amsterdam, The Netherlands,

WOLANSKI, E., MOORE, K., SPAGNOL, S., D'ADAMO, N., and PATTIERATCHI, C. (2001). "Rapid, Human-Induced Siltation of the Macro-Tidal Ord River Estuary, Western Australia." *Estuarine, Coastal and Shelf Science*, Vol. 53, pp. 717-732.

WOLANSKI, E., WILLIAMS, D., SPAGNOL, S., and CHANSON, H. (2004). "Undular Tidal Bore Dynamics in the Daly Estuary, Northern Australia." *Estuarine, Coastal and Shelf Science*, Vol. 60, No. 4, pp. 629-636.

KEEVIL, C.E., CHANSON, H., and REUNGOAT, D. (2015)." Fluid Flow and Sediment Entrainment in the Garonne River Bore and Tidal Bore Collision." *Earth Surface Processes and Landforms*, Vol. 40, No. 12, pp. 1574-1586 (DOI: 10.1002/esp.3735) (ISSN 0197-9337).

Table 1 - Field measurements of tidal bores

Reference	Initial flow V_1 m/s	d_1 m	Instrument	Channel geometry	Remarks
LEWIS (1972)	0 to +0.2	0.9 to 1.4	Hydro-Products™ type 451 current meter	Dee River (UK) near Saltney Ferry footbridge. Trapezoidal channel	Field experiments between March and September 1972.
NAVARRE (1995)	0.65 to 0.7	1.12 to 1.15	Meerestechnik-Electronik GmbH model SM11J acoustic current meter (sampling 10Hz)	Dordogne River (France) at Port de Saint Pardon Width ~ 290 m	Field experiments on 25 & 26 April 1990.
KJERFVE and FERREIRA (1993)			Interocean™ S4 electro-magnetic current meters (sampling: 1-2 Hz)	Rio Mearim (UK)	Field experiments on 19-22 Aug. 1990 & 28 Jan.-2 Feb. 1991.
WOLANSKI et al. (2001)	--	0.45	Analite™ nephelometer	Ord River (East Arm) (Australia) Width ~ 380 m	Field experiments in August 1999.
CHEN (2003)	--	--	--	North Branch of the Changjiang River Estuary (China)	Experiments in April 2001.
SIMPSON et al. (2004)	0.1	~0.8	ADCP (1.2 0 MHz) (sampling rate:1 Hz)	Dee River (UK) near Saltney Ferry Bridge. Trapezoidal channel (base width ~ 60 m)	Field experiments in May and September 2002.
WOLANSKI et al. (2004)	0.15	1.5 to 4	Nortek™ Aquadopp ADCP (sampling rate:2 Hz)	Daly River (Australia). Width ~ 140 m	Field experiments in July and September 2002, and on 2 July 2003.
FAN et al. (2014)	--	--	Sediment cores	Qiatang River (China)	Field works in May 2010.
CHANSON et al. (2011)			ADV Nortek™ Vector (6 MHz) (sampling: 64 Hz)	Arcins channel, Garonne River (France) Width ~ 76 m	Undular tidal bore.
	0.33	1.40 (*)			10 Sept. 2010.
	0.30	1.43 (*)			11 Sept. 2010.
MOUAZE et al. (2010)			ADV Nortek™ Vector (6 MHz) (sampling: 64 Hz)	Pointe du Grouin du Sud, Sélune River (France)	Breaking tidal bore.
	0.86	0.15 (*)			24 Sept. 2010.
	0.59	0.11 (*)			25 Sept. 2010.
FURGEROT et al. (2013)	0.4	0.75	ADV Nortek™ Vector (6 MHz) (sampling: 64 Hz)	Sée River (France) Width ~ 22 m	Undular bore on 7 May 2012.
REUNGOAT et al. (2014a)			microADV Sontek™ (16 MHz) (sampling: 50 Hz)	Arcins channel, Garonne River (France) Width ~ 78 m	Weak undular tidal bore.
	0.68	2.0 (*)			7 June 2012 morning
	0.59	1.94 (*)			7 June 2012 afternoon
Present study	0.26	1.32 (*)	ADV Nortek™ Vectrino+ (10 MHz) (sampling: 200 Hz)	Arcins channel, Garonne River (France) Width ~ 65 m	Undular tidal bore on 19 October 2013 afternoon.

Notes: d_1: initial water depth (at sampling location); V_1: initial flow velocity; (--): information not available; (*): equivalent depth A_1/B_1.

KEEVIL, C.E., CHANSON, H., and REUNGOAT, D. (2015)." Fluid Flow and Sediment Entrainment in the Garonne River Bore and Tidal Bore Collision." *Earth Surface Processes and Landforms*, Vol. 40, No. 12, pp. 1574-1586 (DOI: 10.1002/esp.3735) (ISSN 0197-9337).

Table 2 - Measured properties of sediment samples collected in the Garonne River at Arcins - Comparison with mud samples collected in the Garonne River at Arcins (France) in September 2010 and June 2012 and flood sediment sample during the January 2011 flood of the Brisbane River (Australia)

Ref.	River system	d_{50} μm	d_{90} μm	d_{10} μm	Rheometer	Configuration	Loading	Shear rate Min. 1/s	Shear rate Max. 1/s	Temperature Celsius	Sediment collection data	**s**	τ_c Pa	μ Pa.s	m
Present study	Garonne River at Arcins	15.06	4.13	56.93	Malvern™ Kinexus Pro	Cone 40 mm 4º (smooth)	Continuous ramp	0.01	1,000	25.0	19 October 2013	1.341	6.38	3.13	0.286
													6.21	4.76	0.278
													6.17	5.00	0.271
													6.61	5.31	0.268
													5.48	4.28	0.278
													4.77	4.39	0.276
REUNGOAT et al. (2014a)	Garonne River at Arcins	12.7	3.35	50.0	Malvern™ Kinexus Pro	Cone 40 mm 4º (smooth)	Continuous ramp	0.01	1,000	25.0	7 June 2012	1.357	75.4	36.1	0.22
											8 June 2012	1.428	15.7	11.4	0.27
											8 June 2012		21.5	13.1	0.28
						Disk 20 mm (smooth)	Continuous ramp	0.01	1,000	25.0	7 June 2012	1.357	271	17.5	0.40
											8 June 2012	1.428	74.2	2.87	0.60
CHANSON et al. (2011)	Garonne River at Arcins	--	--	--	TA-ARG2	Cone 40 mm 2º (smooth)	Steady state flow steps	0.01	1,000	20	11 Sept. 2010	1.41	49.7	44.6	0.28
													61.4	52.9	0.27
BROWN and CHANSON (2012)	Brisbane River in flood at Gardens Point Road	26.3	2.96	85.95	Mettler™ Viscosimeter	Cylindrical (0.59 mm between cylinders)		0	1,045	25	14 Jan. 2011	1.46	35.5	8.1	0.34

Notes: d_{50}: median grain size; **s**: specific density; τ_c: apparent yield stress; μ: apparent effective viscosity; m: Herschel-Bulkley law exponent (Eq. (1)).

KEEVIL, C.E., CHANSON, H., and REUNGOAT, D. (2015)." Fluid Flow and Sediment Entrainment in the Garonne River Bore and Tidal Bore Collision." *Earth Surface Processes and Landforms*, Vol. 40, No. 12, pp. 1574-1586 (DOI: 10.1002/esp.3735) (ISSN 0197-9337).

Table 3 - Mean suspended sediment concentration SSC and mean suspended sediment flux per unit area q_s ($kg.s^{-1}.m^{-2}$) during the early flood tide immediately after the Garonne River bore at Arcins

Ref.	River system	Dates	SSC	q_s	Comments
			kg/m^3	$kg.s^{-1}.m^{-2}$	
Present study	Garonne River	19 Oct. 2013	31.55	34.81	Bore passage & 'backward' bore
			13.9	15.21	After 'backward' bore
REUNGOAT et al. (2014a)	Garonne River	7 June 2012	31.7	24.7	
CHANSON et al. (2011)	Garonne River	11 Sept. 2010	46.0	26.3	

KEEVIL, C.E., CHANSON, H., and REUNGOAT, D. (2015)." Fluid Flow and Sediment Entrainment in the Garonne River Bore and Tidal Bore Collision." *Earth Surface Processes and Landforms*, Vol. 40, No. 12, pp. 1574-1586 (DOI: 10.1002/esp.3735) (ISSN 0197-9337).

Fig. 1 - Photographs of tidal bores
(A) Undular tidal bore of the Dordogne River on 24 August 2012 at St Pardon (France)

(B) Qiantang River bore crossing on 6 September 2013 upstream of Daquekou (China), viewed from the left bank: the arrow points to the bore intersection

KEEVIL, C.E., CHANSON, H., and REUNGOAT, D. (2015)." Fluid Flow and Sediment Entrainment in the Garonne River Bore and Tidal Bore Collision." *Earth Surface Processes and Landforms*, Vol. 40, No. 12, pp. 1574-1586 (DOI: 10.1002/esp.3735) (ISSN 0197-9337).

Fig. 2 - Sampling location in the Arcins channel, with surveyed cross-section at low tide water level on 19 October 2013
(A) Tidal bore passing the sampling site - Surfers towards Arcins Island were on the bore front - Sampling carried out from the pontoon fixed on the eastern bank (foreground) of the Arcins Channel

(B) Distorted cross-sectional survey looking upstream (i.e. South) with the eastern/right bank on the left - Comparison with the 2010 and 2012 surveys at the same cross-section and water levels immediately before and after the bore

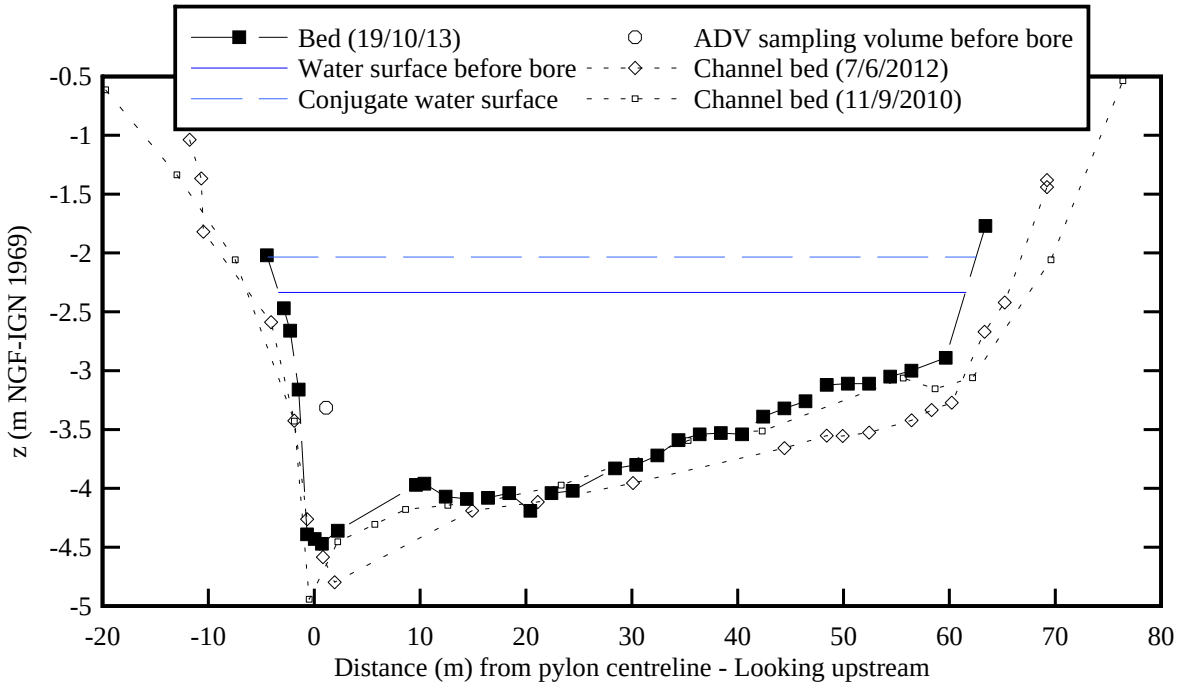

KEEVIL, C.E., CHANSON, H., and REUNGOAT, D. (2015)." Fluid Flow and Sediment Entrainment in the Garonne River Bore and Tidal Bore Collision." *Earth Surface Processes and Landforms*, Vol. 40, No. 12, pp. 1574-1586 (DOI: 10.1002/esp.3735) (ISSN 0197-9337).

Fig. 2 - Sampling location in the Arcins channel, with surveyed cross-section at low tide water level on 19 October 2013
(C) Un-distorted dimensioned sketch of the ADV mounting, sampling volume location and water surface 5 minutes prior to the tidal bore on 19 October 2013- Left: view from Arcins Island - Right: looking upstream (i.e. South)

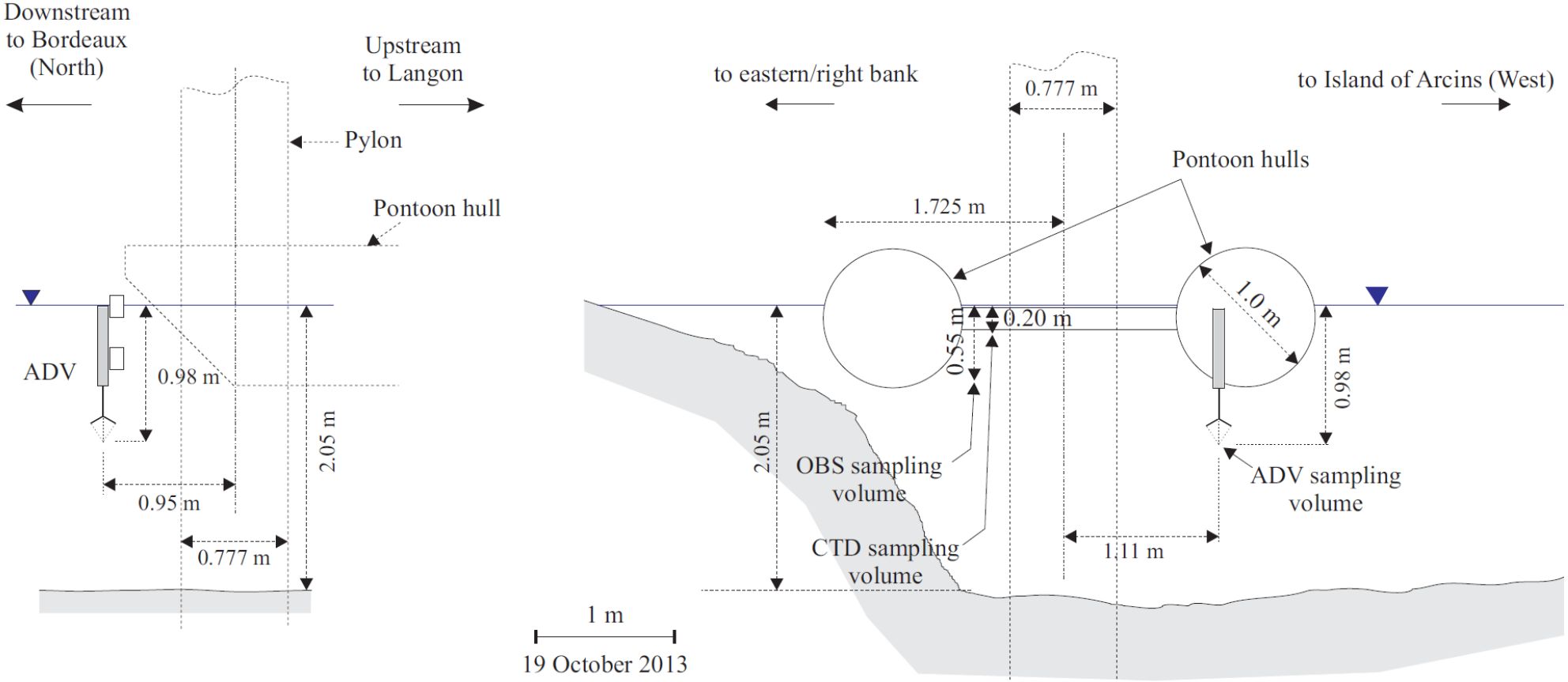

KEEVIL, C.E., CHANSON, H., and REUNGOAT, D. (2015)." Fluid Flow and Sediment Entrainment in the Garonne River Bore and Tidal Bore Collision." *Earth Surface Processes and Landforms*, Vol. 40, No. 12, pp. 1574-1586 (DOI: 10.1002/esp.3735) (ISSN 0197-9337).

Fig. 3 - Plan view of the tidal bore propagation around the Arcins Island including formation of the 'backward' bore on 19 October 2013 - Right: top view cartoon of bore propagation around the island

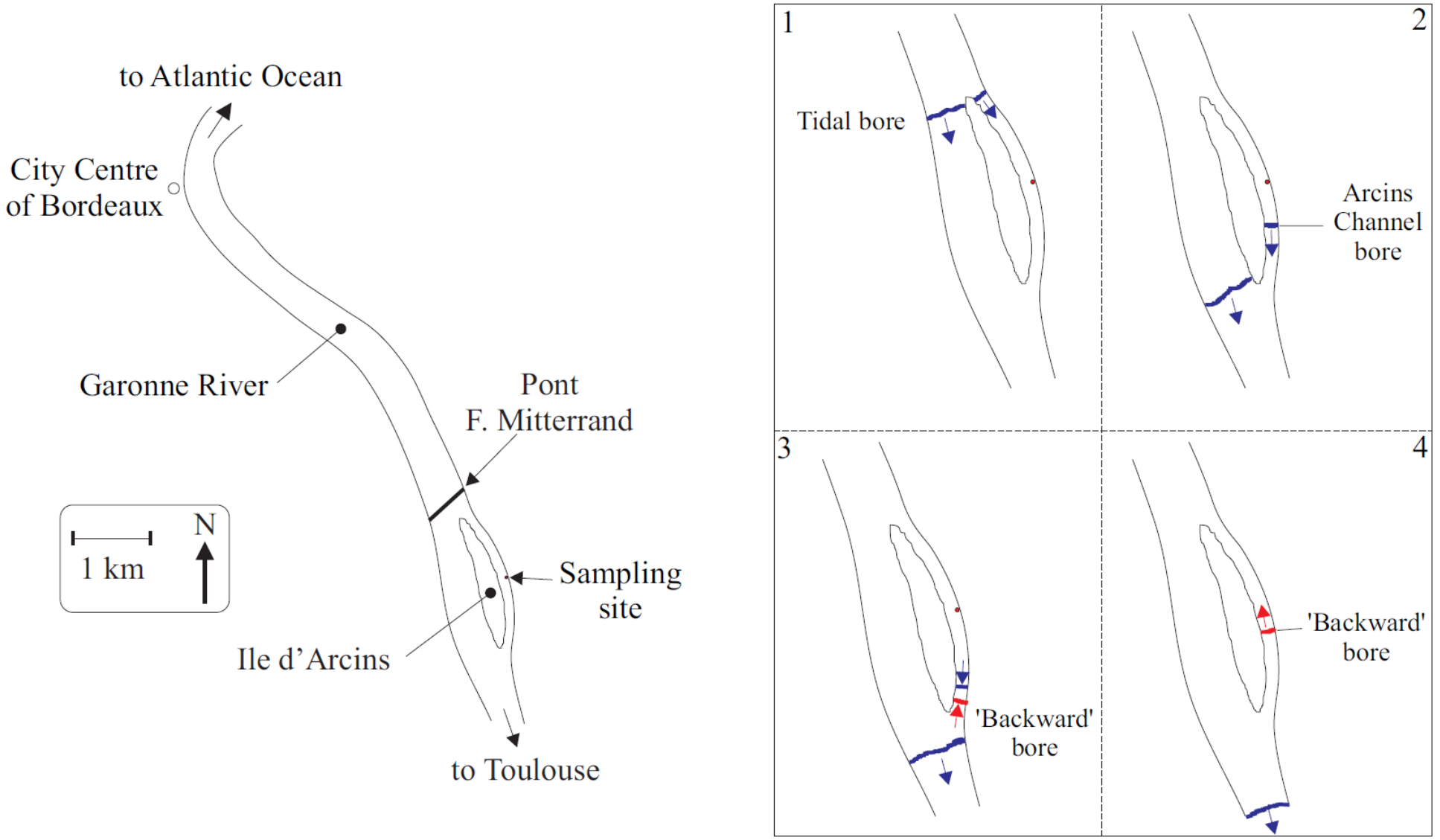

KEEVIL, C.E., CHANSON, H., and REUNGOAT, D. (2015)." Fluid Flow and Sediment Entrainment in the Garonne River Bore and Tidal Bore Collision." *Earth Surface Processes and Landforms*, Vol. 40, No. 12, pp. 1574-1586 (DOI: 10.1002/esp.3735) (ISSN 0197-9337).

Fig. 4 - Relationship between suspended sediment concentration and backscatter amplitude for the sediment samples collected in the Arcins channel on 19 and 20 October 2013 - Comparison between laboratory data (Bordeaux, Leeds) and sediment-laden water samples collected on 19 October 2013 (coloured symbols with error bars)

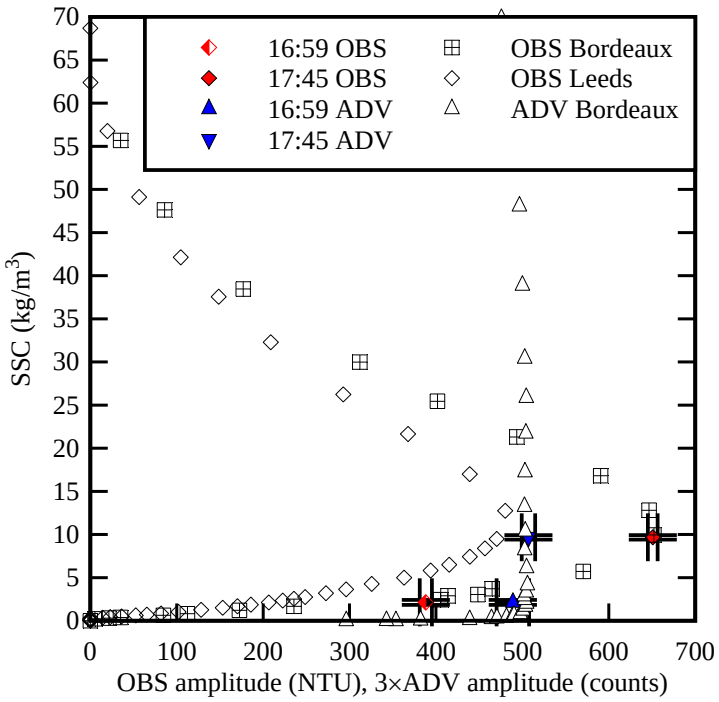

KEEVIL, C.E., CHANSON, H., and REUNGOAT, D. (2015)." Fluid Flow and Sediment Entrainment in the Garonne River Bore and Tidal Bore Collision." *Earth Surface Processes and Landforms*, Vol. 40, No. 12, pp. 1574-1586 (DOI: 10.1002/esp.3735) (ISSN 0197-9337).

Fig. 5 - Tidal bore of the Garonne River in the Arcins channel on 19 October 2013
(A) Approaching bore, looking downstream about 17:06 (white arrows points to longitudinal bed forms); (B) Upstream propagation of undular bore at 17:07; (C) Tidal bore collision at 17:10:15; (D) Upstream propagation of 'backward' bore (white arrow) of the Garonne River in the Arcins channel at 17:15:13

(A) (B)

(C)

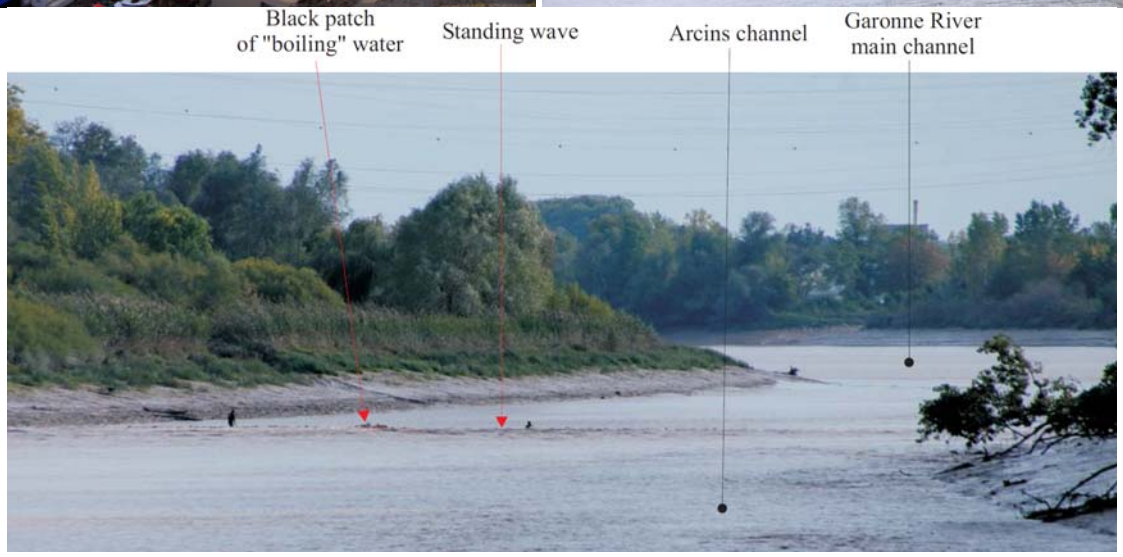

(D)

KEEVIL, C.E., CHANSON, H., and REUNGOAT, D. (2015)." Fluid Flow and Sediment Entrainment in the Garonne River Bore and Tidal Bore Collision." *Earth Surface Processes and Landforms*, Vol. 40, No. 12, pp. 1574-1586 (DOI: 10.1002/esp.3735) (ISSN 0197-9337).

Fig. 6 - Time variations of instantaneous longitudinal velocity component and water depth in the Arcins channel on 19 October 2013 - Post-processed ADV data (sampling rate: 200 Hz) and surface velocity on the channel centreline - Dashed lines mark the passage of the tidal bore and 'backward' bore

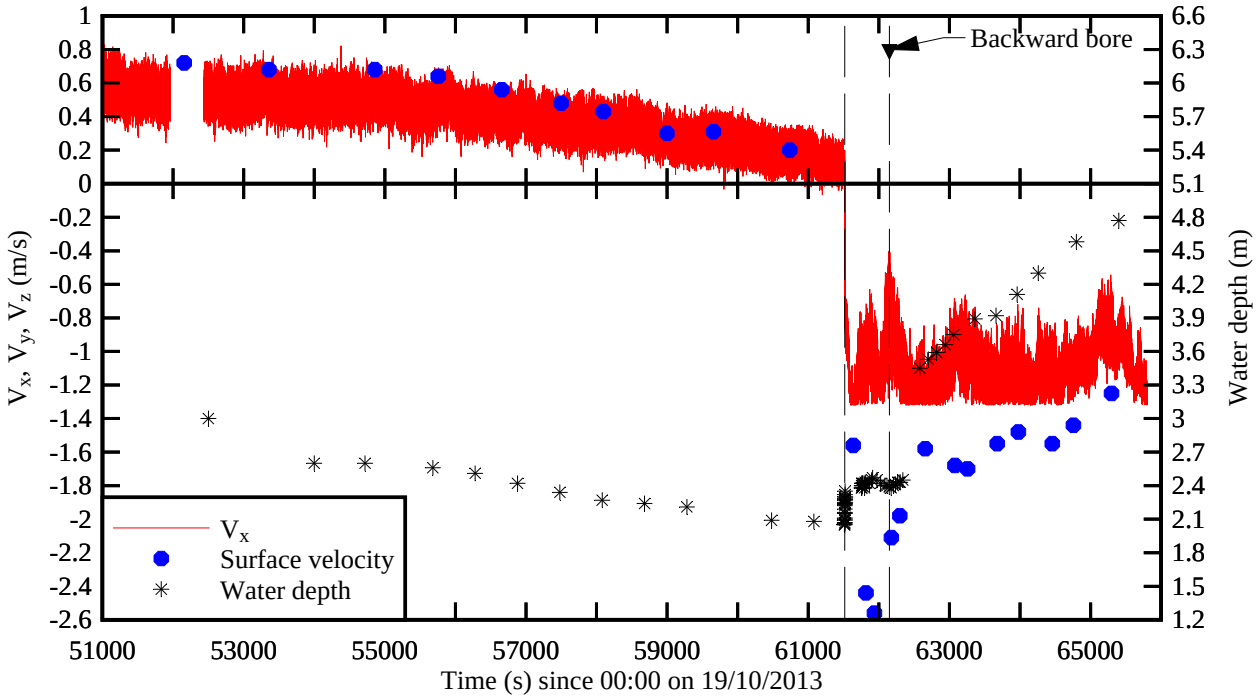

KEEVIL, C.E., CHANSON, H., and REUNGOAT, D. (2015)." Fluid Flow and Sediment Entrainment in the Garonne River Bore and Tidal Bore Collision." *Earth Surface Processes and Landforms*, Vol. 40, No. 12, pp. 1574-1586 (DOI: 10.1002/esp.3735) (ISSN 0197-9337).

Fig. 7 - Time-variations of Reynolds stresses and water depth during the tidal bore passage on 19 October 2013 - Post-processed ADV data, sampling rate: 200 Hz - Dashed lines mark the passage of the tidal bore and 'backward' bore

(A) $\rho \times v_x^2$ and $\rho \times v_x \times v_y$

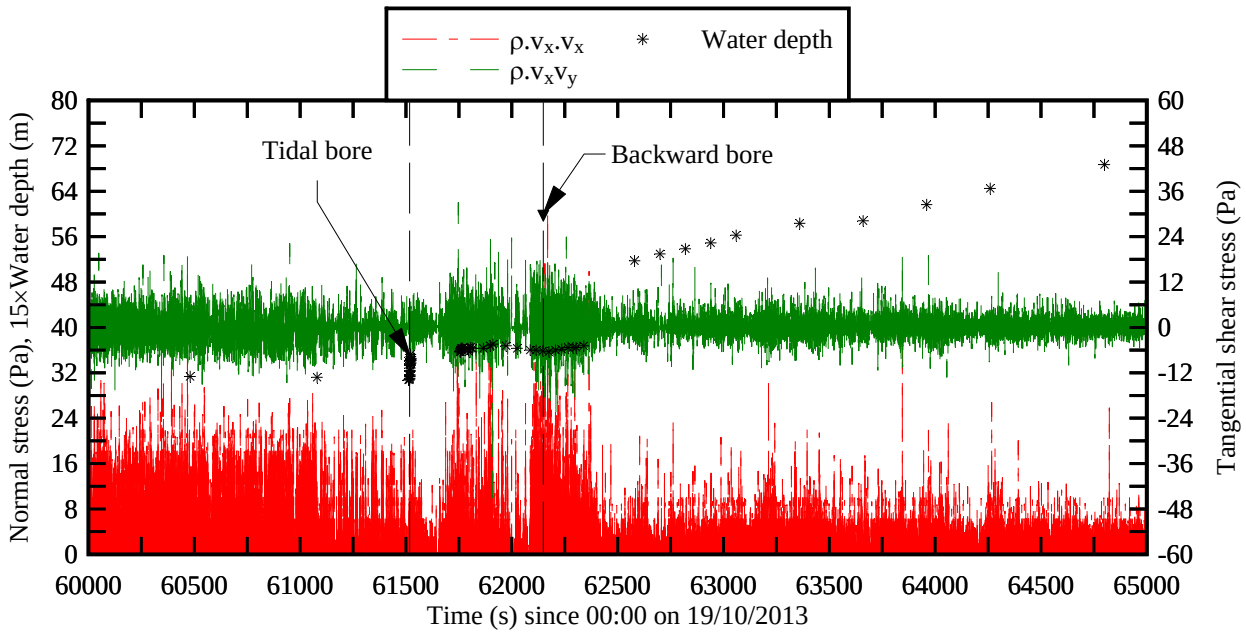

(B) $\rho \times v_z^2$ and $\rho \times v_x \times v_z$

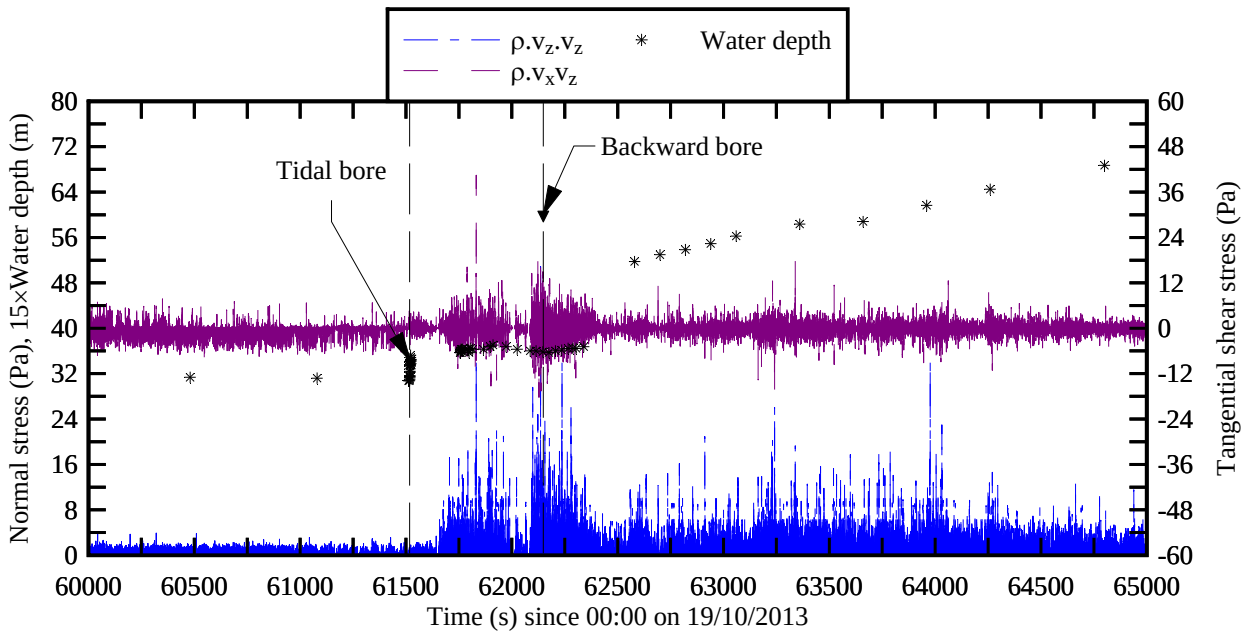

KEEVIL, C.E., CHANSON, H., and REUNGOAT, D. (2015)." Fluid Flow and Sediment Entrainment in the Garonne River Bore and Tidal Bore Collision." *Earth Surface Processes and Landforms*, Vol. 40, No. 12, pp. 1574-1586 (DOI: 10.1002/esp.3735) (ISSN 0197-9337).

Fig. 8 - Time variations of suspended sediment concentration (SSC) estimate, mean suspended sediment flux per unit area and water depth on 19 October 2013 - Median OBS data for 5 s and ADV data averaged over 5 s, all data returned every 10 s - Dashed lines mark the passage of the tidal bore and 'backward' bore
(A) Time variations of suspended sediment concentration (SSC) estimate - Comparison with sediment-laden water sample data

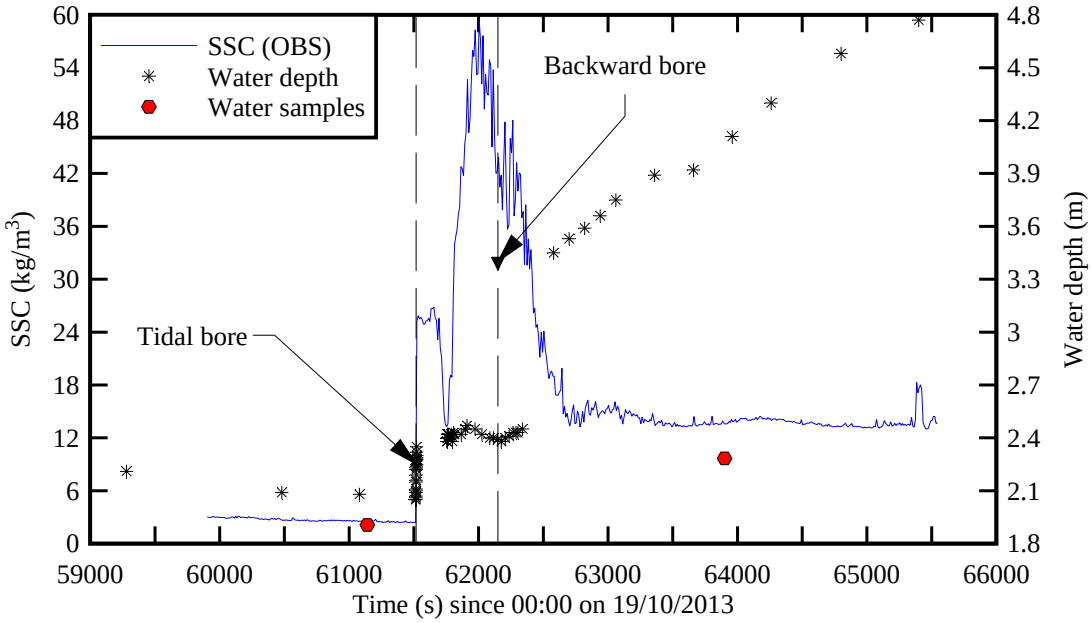

(B) Time variations of the mean suspended sediment flux per unit area (q_s = SSC×V_x)